ELSEVIER

Journal of Chromatography A, 769 (1997) 25–35

JOURNAL OF CHROMATOGRAPHY A

Modeling, simulation and operation of a simulated moving bed for continuous chromatographic separation of 1,1′-bi-2-naphthol enantiomers

Luís S. Pais, José M. Loureiro, Alírio E. Rodrigues*

Laboratory of Separation and Reaction Engineering, Faculty of Engineering, University of Porto, Rua dos Bragas, 4099 Porto Codex, Portugal

Abstract

The objective of this paper is to study the separation of enantiomers of 1,1′-bi-2-naphthol in 3,5-dinitrobenzoyl phenylglycine bonded to silica gel, using heptane–isopropanol (72:28) as eluent by simulated moving bed chromatography (SMB). A model for the prediction of the cyclic steady state performance of the SMB, based on the analogy with the true moving bed, is developed assuming axial dispersion flow, linear driving force approximation for intraparticle mass transfer and multicomponent adsorption equilibria. The SMB package allows the simulation of the pilot unit. The effect of several operating parameters on the SMB performance is analyzed. The performance is characterized by purity, recovery, solvent consumption and adsorbent productivity. The package is an important tool for learning and training operators, allowing the choice of best operating conditions. The operation of the SMB pilot unit was carried out for the separation of racemic mixtures using a 8-column configuration. Purities and recoveries higher than 95% in the extract and raffinate were obtained. Model and experimental results are compared and the package is also used to predict the steady state internal profiles for the SMB operation in good agreement with experimental results.

Keywords: Simulated moving bed chromatography; Enantiomer separation; Computer simulation; Binaphthol

1. Introduction

The concept of simulated moving bed (SMB) technology has been known since 1961 when the first patent by Broughton appeared [1]. The heart of the SMB technology is a rotary valve which periodically changes the position of feed, eluent, extract and raffinate lines along the bed. In this way the solid movement in a true moving bed (TMB) is simulated.

The SMB technology, developed by UOP, has been used in the chemical industry for several separations known as Sorbex processes [2–4]. They include the Parex process for separation of *p*-xylene from a mixture of C_8 aromatics, the Molex process for the extraction of normal paraffins from branched and cyclic hydrocarbons, the Olex process to separate olefins from paraffins and the Sarex process for the recovery of fructose from fructose–glucose mixtures in the production of high fructose corn syrup HFCS [5–8].

The SMB technology has found new applications in the areas of biotechnology, pharmaceuticals and fine chemistry [9]. Pilot and industrial SMB for such applications have been developed by UOP [10,11] and Separex [12]. It should be pointed out that scaling down of the Sorbex flowsheet becomes less

*Corresponding author.

PII S0021-9673(96)01076-X

economical than using a system of individual beds segmented by valves and feed and product lines [13].

More recent applications are related with chiral technology. The need for the separation of enantiomers for pharmaceutical applications is increasing as regulatory aspects become more stringent. It is well known that isomers can have different therapeutical values and therefore enantiomeric resolution is an important issue particularly in health-related fields [14]. The separation of enantiomers by conventional techniques is difficult because separation factors are low. Continuous chromatography and particularly SMB technology is appropriate, provided chromatographic phases for enantiomer separation are available [15,16]. Continuous chromatography in SMB also eliminates drawbacks of batch chromatography, namely dilution of species and low adsorbent utilization [17,18]. Examples of enantiomers separations have been reported: 1-phenylethanol [19], praziquantel [20], 3-chloro-1-phenylpropanol [21], D,L-threonine [22], 1*a*,2,7,7*a*-tetrahydro-3-methoxynaphtha[2,3*b*]oxirane [23–26] and binaphthol enantiomers [27].

The objective of this paper is to study the separation of enantiomers of 1,1′-bi-2-naphthol in 3,5-dinitrobenzoyl phenylglycine bonded to silica gel columns using heptane–isopropanol (72:28) as eluent by using SMB chromatography.

The work involves the following steps: (i) development of a model for the SMB and numerical solution of model equations; (ii) understanding SMB process by using the simulation package to predict the effect of operating variables on the SMB performance; (iii) operation of the SMB pilot unit for the bi naphthol system and comparison with simulated results.

2. Modeling of a simulated moving bed

2.1. True moving bed strategy of modeling

Models available in literature for SMB separation processes have been summarized by Ruthven and Ching [28]. There are two main strategies of modeling SMB processes: one represents the real SMB and the other the equivalent TMB. The model used in this work for the prediction of the cyclic steady state performance of the SMB was developed based on the

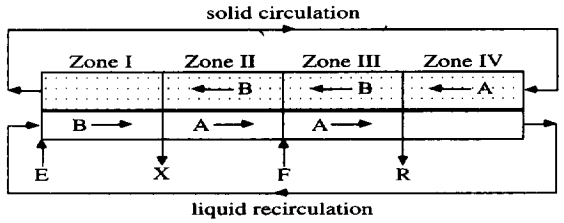

Fig. 1. Schematic diagram of the four-section TMB.

analogy with the true moving bed. In the four-section TMB approach, shown in Fig. 1, the liquid and the solid-phases flow in opposite directions. The liquid flowing out of zone IV is recycled to zone I while the solid coming out of zone I is recycled to zone IV. The inlet and outlet lines (eluent, extract, feed and raffinate) divide the system into four zones, each performing a specific function. Zone I, between eluent and extract nodes, allows solid regeneration. Its function is the desorption of the more retained species B from the solid-phase. In Zone II, between extract and feed nodes, desorption of the less retained species A takes place. Zone III, between feed and raffinate nodes, is the zone of adsorption of the more retained component B. Finally, zone IV, between raffinate and eluent nodes, is the zone of eluent regeneration. Its function is the adsorption of the less retained component A.

The design problem of a TMB consists on setting the liquid flow-rates in each zone and the solid flow-rate as well to obtain the desired separation. Some constraints have to be met if one wants to recover the less adsorbed component A in the raffinate and the more retained component B in the extract. These constraints are expressed in terms of net fluxes of components in each zone. In zone I the heavier species B must move upwards, in zone II the light species must move upwards, in zone III the net flux of B must be downwards and in zone IV the net flux of A has to be downwards, i.e.,

$$\frac{Q_{\mathrm{I}}c_{\mathrm{B\,I}}}{Q_{\mathrm{S}}q_{\mathrm{B\,I}}} > 1;\ \frac{Q_{\mathrm{II}}c_{\mathrm{A\,II}}}{Q_{\mathrm{S}}q_{\mathrm{A\,II}}} > 1 \text{ and } \frac{Q_{\mathrm{II}}c_{\mathrm{B\,II}}}{Q_{\mathrm{S}}q_{\mathrm{B\,II}}} < 1;$$
$$\frac{Q_{\mathrm{III}}c_{\mathrm{A\,III}}}{Q_{\mathrm{S}}q_{\mathrm{A\,III}}} > 1 \text{ and } \frac{Q_{\mathrm{III}}c_{\mathrm{B\,III}}}{Q_{\mathrm{S}}q_{\mathrm{B\,III}}} < 1;$$
$$\frac{Q_{\mathrm{IV}}c_{\mathrm{A\,IV}}}{Q_{\mathrm{S}}q_{\mathrm{A\,IV}}} < 1 \qquad (1)$$

where Q_{I}, Q_{II}, Q_{III}, Q_{IV} are the volumetric liquid

flow-rates in the various zones of the TMB, Q_S is the solid flow-rate, c_{Aj}, c_{Bj} are the concentrations of species A and B in the liquid phase and q_{Aj}, q_{Bj} are the adsorbed concentrations of components A and B, in zone j.

The same constraints can be expressed alternatively in terms of fluid and solid velocities. Defining the dimensionless parameter:

$$\gamma^*_{ij} = \gamma_j \frac{\varepsilon}{(1-\varepsilon)} \frac{c_{ij}}{q_{ij}} \quad (2)$$

where $\gamma_j = v_j / u_s$ is the ratio between fluid and solid velocities in zone j and $\varepsilon/(1-\varepsilon)$ is the ratio between fluid and solid volumes, the constraints defined by Eq. (1) becomes:

$$\gamma^*_{B\,I} > 1;\ \gamma^*_{A\,II} > 1 \text{ and } \gamma^*_{B\,II} < 1;\ \gamma^*_{A\,III} > 1 \text{ and } \gamma^*_{B\,III} < 1;\ \gamma^*_{A\,IV} < 1 \quad (3)$$

The package developed allows the study of the transient TMB based on a model which considers axial dispersion flow for the bulk fluid phase, linear driving force (LDF) for the intraparticle mass transfer rate and takes into account multicomponent adsorption equilibria. However, for the cyclic steady state performance of a SMB only TMB steady state is needed. Model equations were presented elsewhere [27] and are summarized in Table 1. The model parameters are:

$\frac{(1-\varepsilon)}{\varepsilon}$ Ratio between solid and fluid volumes

$\gamma_j = \frac{v_j}{u_s}$ Ratio between fluid and solid velocities

$\mathrm{Pe}_j = \frac{v_j L_j}{D_{L_j}}$ Peclet number

$\alpha_j = \frac{kL_j}{u_s}$ Number of intraparticle mass transfer units

Adsorption equilibrium parameters have to be added to the list above.

2.2. Process performance criteria

The SMB performance is characterized by four process parameters: purity, recovery, solvent consumption and adsorbent productivity. For the case of a binary separation in which the less retained species A is recovered in the raffinate, and the more retained component B is recovered in the extract, process performance parameters are defined in Table 2. When a racemic mixture is considered, $C_F^A = C_F^B$; then SCX = SCR·RCR/RCX and PRX = PRR·RCX/RCR.

Table 1
Model equations for the transient TMB

Mass balance in a volume element of the bed

$$\varepsilon D_{L_j} \frac{\partial^2 c_{ij}}{\partial z^2} - \varepsilon v_j \frac{\partial c_{ij}}{\partial z} + (1-\varepsilon) u_s \frac{\partial q_{ij}}{\partial z} = \varepsilon \frac{\partial c_{ij}}{\partial t} + (1-\varepsilon) \frac{\partial q_{ij}}{\partial t}$$

Mass balance in the particle

$$u_s \frac{\partial q_{ij}}{\partial z} + k(q^*_{ij} - q_{ij}) = \frac{\partial q_{ij}}{\partial t}$$

Initial conditions

$t = 0$: $\quad c_{ij} = q_{ij} = 0$

Boundary conditions

$z = 0$: $\quad c_{ij} - \frac{D_{L_j}}{v_j} \frac{dc_{ij}}{dz} = c_{ij,0}$

$z = L_j$ $\quad \frac{dc_{ij}}{dz} = 0$ and $q_{ij} = q_{ij+1,0}$

Multicomponent adsorption equilibrium isotherm

$q^*_{Aj} = f_A(c_{Aj}, c_{Bj})$ and $\quad q^*_{Bj} = f_B(c_{Aj}, c_{Bj})$

Mass balances at the nodes of the inlet and outlet lines of the TMB

Eluent node: $\quad c_{i1,0} = \frac{v_{IV}}{v_I} c_{iIV,L_{IV}}$

Extract node: $\quad c_{iII,0} = c_{i1,L_I}$

Feed node: $\quad c_{iIII,0} = \frac{v_{II}}{v_{III}} c_{iII,L_{II}} + \frac{v_F}{v_{III}} c_i^F$

Raffinate node: $\quad c_{iIV,0} = c_{iIII,L_{III}}$

i = A, B refers to the species in the mixture.
j = I, II, III, IV is the zone number.

3. Simulation results

The effect of several operating parameters on the SMB performance for the bi naphthol separation was

Table 2
SMB Performance criteria

Performance Parameter	Extract	Raffinate
Purity (%)	$100\ C_X^B/(C_X^A+C_X^B)$	$100\ C_R^A/(C_R^A+C_R^B)$
Recovery (%)	$100\ C_X^B Q_X/(C_F^B Q_F)$	$100\ C_R^A Q_R/(C_F^A Q_F)$
Solvent Consumption (l/g)	$(Q_E+Q_F)/C_X^B Q_X)$	$(Q_E+Q_F)/(C_R^A Q_R)$
Productivity (g/h l of solid)	$C_X^B Q_X/V_S$	$C_R^A Q_R/V_S$

analyzed. The adsorption equilibrium isotherm proposed by the Separex group [29,30] of bi-Langmuir type was used:

$$q_A^* = \frac{2.69c_A}{1+0.0336c_A+0.0466c_B} + \frac{0.10c_A}{1+c_A+3c_B} \quad (4a)$$

$$q_B^* = \frac{3.73c_B}{1+0.0336c_A+0.0466c_B} + \frac{0.30c_B}{1+c_A+3c_B} \quad (4b)$$

The resulting model equations, described by a set of PDEs, were numerically solved by using the Pdecol package [31] based on the method of orthogonal collocation in finite elements.

The conditions of a complete separation were defined in terms of the γ_j model parameters, which are directly related with the SMB operating variables (fluid and solid velocities in the four zones of the SMB unit). From the four constraints presented in Eqs. (1,3) those related to zones II and III play the crucial role on the separation performance of the SMB [32]. Taking into account this consideration, a region of complete separation in a $\gamma_{III}-\gamma_{II}$ plane can be defined.

The first case studied concerns the situation where axial dispersion and mass transfer resistance are negligible. A similar study was done by Storti and coworkers [32–34] in the frame of equilibrium theory, where mass transfer resistances and axial dispersion were neglected. The value for mass transfer coefficient used in this case was $k=0.5\ s^{-1}$ ($\alpha=180$). The $\gamma_{III}-\gamma_{II}$ plot was built keeping constant the recycling flow-rate and the rotation period (and so γ_{IV}). The total inlet or outlet flow-rates were kept constant in all simulations and equal to 25.09 ml/min. Other operating conditions and model parameters are summarized in Table 3.

Fig. 2 shows the $\gamma_{III}-\gamma_{II}$ plot obtained for the first case where four regions are defined: a region of complete separation, two regions where only one outlet stream is 100% pure and a last region where neither of them is 100% pure. Considering that the constraints concerning zones I and IV are fulfilled, the $\gamma_{III}-\gamma_{II}$ plot is an important tool in the choice of best operating conditions. The closed circles are numerical results based on the equivalence between the TMB and the SMB; the thick lines connect those results. The thin line in Fig. 2 has two branches. The diagonal $\gamma_{III}=\gamma_{II}$ corresponds to zero feed flow-rate; therefore, γ_{III} must be higher than γ_{II}. The horizontal branch $\gamma_{III}\approx 3.760$ corresponds to zero raffinate flow-rate; in this case, the extract flow-rate is 25.09 ml/min.

The effects of the extract (or raffinate) and feed (or eluent) flow-rates on the SMB performance were also studied. Fig. 3 presents the lines in the $\gamma_{III}-\gamma_{II}$

Table 3
Operating conditions and model parameters for the $\gamma_{III}-\gamma_{II}$ plot with mass transfer coefficient, $k=0.5\ s^{-1}$

SMB operation conditions	Model parameters
Feed concentration: 2.9 g/l each	Solid/fluid volumes, $(1-\varepsilon)/\varepsilon=1.5$
Rotation period: 3 min	Number of mass transfer units, $\alpha=180$
Recycling flow-rate: 35.38 ml/min	Peclet number, $Pe=2000$
Column diameter: 2.6 cm	Ratio between fluid and solid velocities
Zone length: 21.0 cm	in zone IV: $\gamma_{IV}=3.760$

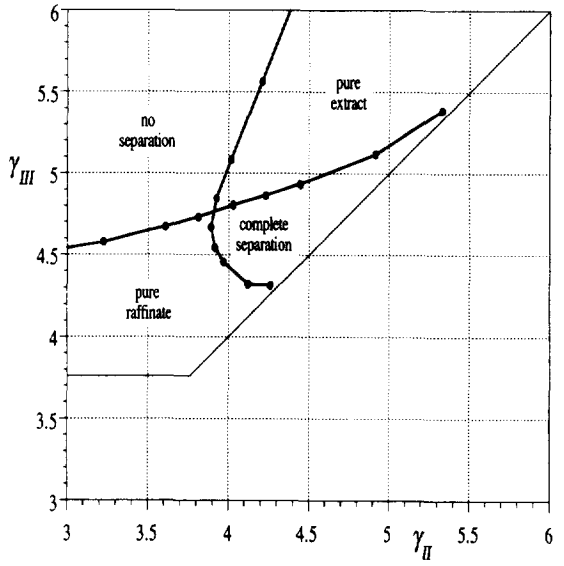

Fig. 2. Regions of operation of the TMB in a plot of the ratio of fluid/solid velocities in zone III (γ_{III}) vs. ratio of fluid/solid velocities in zone II (γ_{II}); the closed circles represent numerical simulation results for negligible mass transfer resistance, $k=0.5$ s^{-1}; other conditions are shown in Table 3.

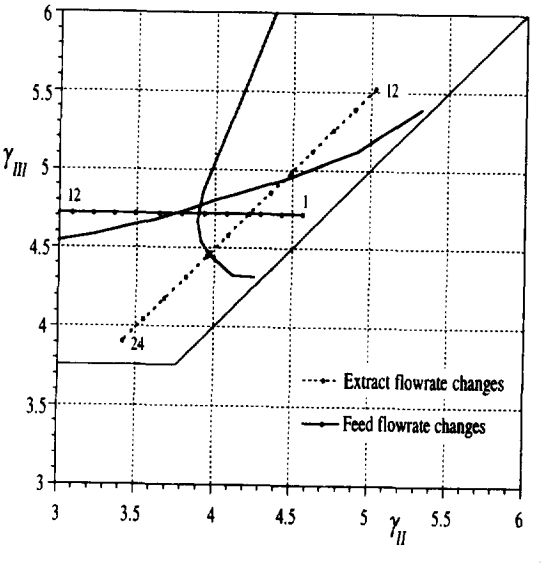

Fig. 3. Effect of extract (12–24 ml/min) and feed (1–12 ml/min) flow-rate changes on the region of operation of TMB shown in the γ_{III}–γ_{II} plot; data as in Fig. 2.

plot, describing the effect of changes in extract and feed flow-rates. In the study of the effect of the extract flow-rate, feed and eluent flow-rates were kept constant and equal to 3.64 and 21.45 ml/min, respectively. In the study of the effect of the feed flow-rate, extract and raffinate flow-rates were kept constant and equal to 18.00 and 7.09 ml/min, respectively. The other operating conditions and model parameters used were those presented in Table 3.

The influence of the extract flow-rate on the SMB performance is shown in Fig. 4. Comparing them to Fig. 3, we can observe a central region where complete separation is achieved and two adjacent regions where only one outlet is 100% pure. The deviation of the value of the extract flow-rate from its central region affects the performance of one or the other enantiomer, depending on which direction the extract flow-rate is changed. For example, increasing the extract flow-rate will lead to a lower liquid flow-rate in the second zone and its constraint is eventually not obeyed. Therefore, species A will have a net flux downwards and will contaminate the extract with decrease of purity in that stream.

The influence of the feed flow-rate on the SMB performance is shown in Fig. 5. Increasing the feed flow-rate improve productivity and solvent consumption but reduce both purity and recovery.

If mass transfer resistance is important, we may not obtain a region of 100% purity for both enantiomers. This case is illustrated using the same operating conditions and model parameters of the previous one, except that the mass transfer coefficient is now $k=0.1$ s^{-1} ($\alpha=36$). Fig. 6 shows the γ_{III}–γ_{II} plot obtained for this case where the four regions (A, B, C and D) described before are defined in terms of 99%, 95% and 90% purity criteria. In region A, there is no separation; in region B, the raffinate purity is at least 90% when the dashed line (open circles) is used as border and at least 95% when the full line (closed circles) is used instead, whereas the extract purity is lower than those values; in region C, both the raffinate and the extract have at least 99%, 95% or 90% according to the lines used as borders (identified by closed triangles, closed circles and open circles, respectively); in region D, the extract purity is at least 90% or 95% accordingly with the line used as border (dashed or full, respectively), whereas the raffinate purity is inferior to those values.

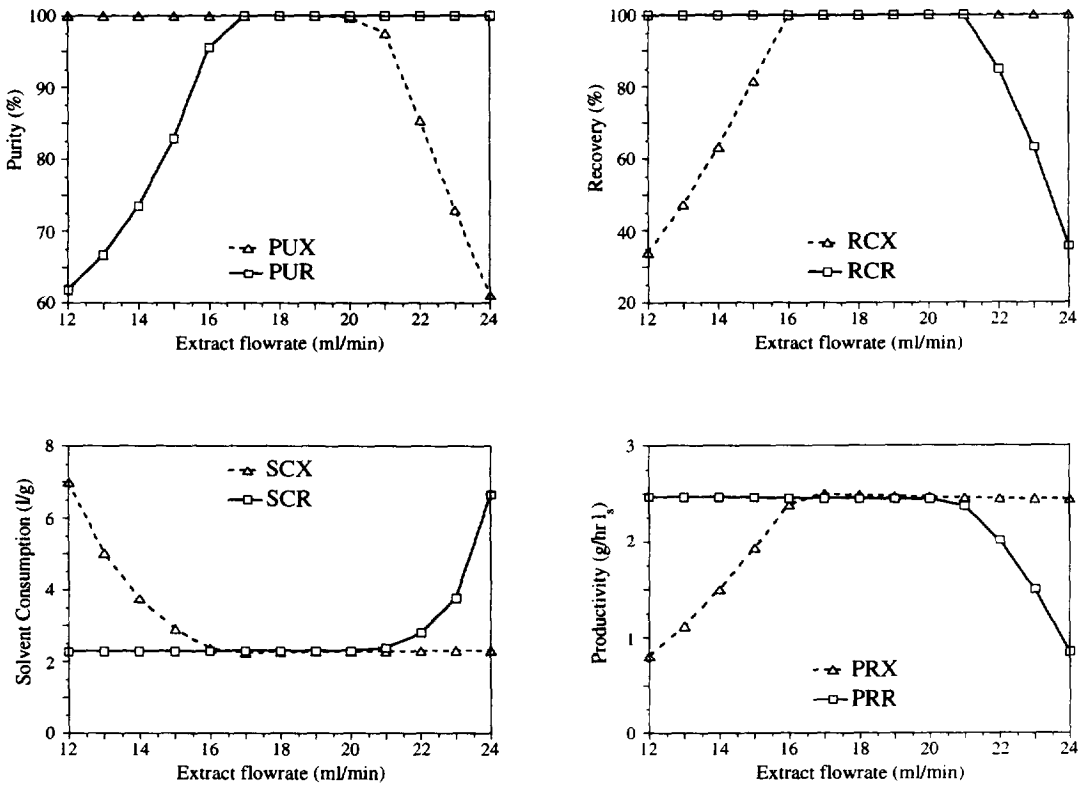

Fig. 4. Effect of the extract flow-rate on the performance parameters (purity, recovery, solvent consumption and productivity), for the conditions shown in Table 3.

4. Operation of the simulated moving bed

4.1. SMB pilot unit

The SMB pilot unit used in this work is the Licosep 12-26, developed by Separex (Champigneulles, France) in cooperation with the Institut Français du Pétrole. It is a continuous chromatographic system constituted by 12 columns connected in series. The columns are Superformance 300-26 (Merck, Darmstadt, Germany) with 26 mm internal diameter and adjustable length (5–20 cm). They have a jacket which allows operation of the SMB up to 60°C. Each column is connected with four lines (eluent, feed, extract and raffinate lines) and 48 two-way high-pressure pneumatic valves (TOP Industrie, France) allow the connection of the inlet-outlet lines of the columns. A three-head membrane pump (Milroyal, Pont St. Pierre, France) is used for the recycle flow. The other flows (eluent, feed, extract and raffinate) are controlled by four pumps Merck–Hitachi (Darmstadt, Germany), connected to the computer via RS 232 interface. The system temperature is measured and controlled through a thermostatic bath. The SMB unit can stand pressures up to 60 bar. The SMB pilot is controlled by a central system using the Licosep control software.

4.2. SMB operation

The operation of the SMB pilot for the bi naphthol enantiomers (molecular mass $M_r = 286.3$) purification was carried out using a 8-column configuration. Columns are made of 3,5-dinitrobenzoyl phenylglycine bonded to silica gel (Merck). Each column is 10.5 cm long. Silica particles have diameter in the range 25 to 40 μm. The eluent used was heptane–isopropanol (72:28, v/v). Operation temperature was

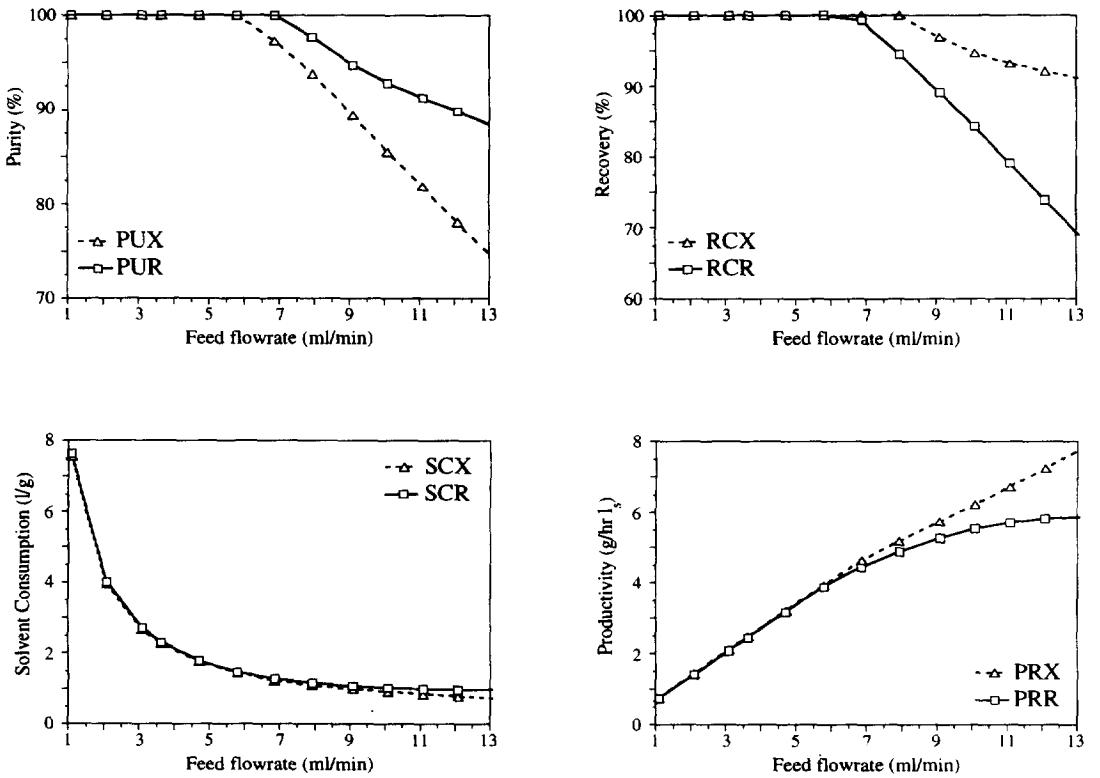

Fig. 5. Effect of the feed flow-rate on the performance parameters (purity, recovery, solvent consumption and productivity), for the conditions shown in Table 3.

fixed at 25°C and the total pressure drop was 20 bar for an average flow-rate of 40 ml/min.

The samples collected were analyzed in a HPLC system (Gilson, Villiers le Bel, France) using a 250 mm×4 mm column filled with 5 μm poly-N-acryloyl-(*S*)-phenylalanine diethylamide as stationary phase. The eluent was the same mixture of heptane–isopropanol and outlet concentration was followed by UV detection at 254 nm.

Four runs were carried out using a configuration of two columns per zone, with the experimental conditions presented in Table 4. The experimental performance parameters were determined by analysis of the extract and raffinate samples collected during a whole cycle after cyclic steady state was achieved. The experimental performance parameters are shown in Table 5. For a rotation period of 2.80 min, purities and recoveries higher than 95% can be obtained in the extract and raffinate. For the same conditions, the model predicted purities for the extract and raffinate were 76.8 and 92.3% for run A, 95.4 and 97.6% for run B, 97.4 and 98.2% for run C and 97.9 and 85.8% for run D, respectively. Model and experimental results are compared in the γ_{III}–γ_{II} plot for $k=0.1$ s^{-1} with good agreement (Fig. 7).

Other runs were carried out to study the effect of the configuration in the SMB performance. The configurations tested were 2222 (two columns per zone) for run 1, 1331 for run 2 and 1241 for run 3. The experimental conditions were the same of the previous runs (see Table 4), except the value for the rotation period that is now 2.75 min for all the configurations. Although no specific optimization was made for each configuration, no significant differences were observed in the SMB performance parameters between the three configurations studied (Table 6). The internal profiles were measured using the 6-port valve of the Licosep SMB pilot to withdraw samples from the system. The samples were collected at each half-time period and after

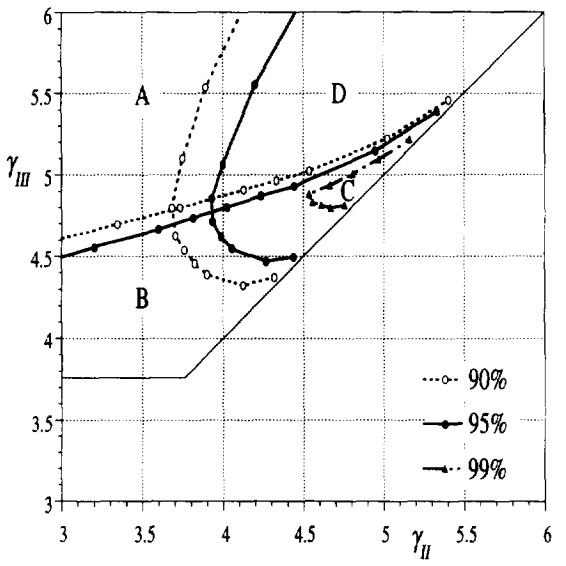

Fig. 6. Regions of operation of the TMB in a γ_{III}–γ_{II} plot for $k=0.1$ s^{-1}: (A) no separation; (B) raffinate purity of at least 90% (○) or 95% (●); (C) raffinate and extract purities of at least 90% (○), 95% (●) or 99% (▲); (D) extract purity of at least 90% (○) or 95% (●).

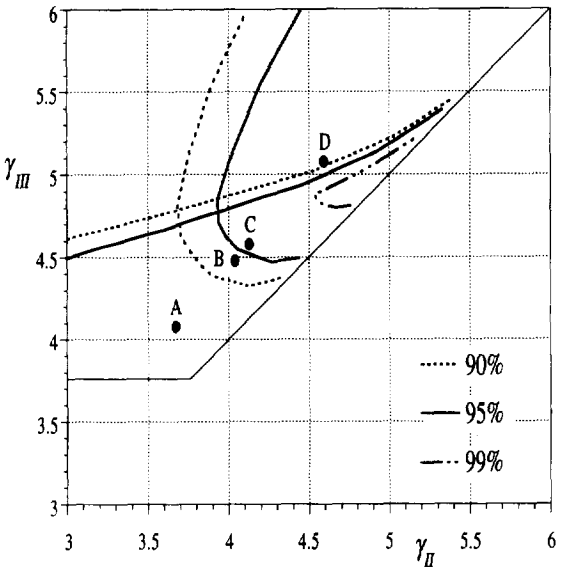

Fig. 7. Experimental results for the runs A, B, C and D (conditions shown in Table 4) displayed in the respective regions of the γ_{III}–γ_{II} plot.

Table 4
Experimental conditions for the bi-naphthol system

Run	A	B	C	D
Feed concentration, g/l each		2.9		
Recycling flow-rate, ml/min		35.38		
Eluent flow-rate, ml/min		21.45		
Extract flow-rate, ml/min		16.00		
Feed flow-rate, ml/min		3.64		
Raffinate flow-rate, ml/min		9.09		
Rotation period, min	2.55	2.75	2.80	3.05
γ_I	5.50	6.01	6.14	6.77
γ_{II}	3.67	4.04	4.13	4.59
γ_{III}	4.08	4.48	4.58	5.08
γ_{IV}	3.04	3.36	3.44	3.84

cyclic steady state was achieved. Fig. 8 shows the SMB experimental internal profiles at cyclic steady state for the three configurations. Simulated results are also displayed using $k=0.1$ s^{-1} (symbols are experimental results, lines for model simulation). For the same conditions, the model predicted purities for the extract and raffinate were 95.4 and 97.6% for run 1, 97.0 and 94.5% for run 2 and 94.6 and 94.3% for run 3, respectively. The agreement between model and experimental results is reasonable except for the concentration of the more retained component B in the second zone.

Table 5
Experimental performance parameters for the four runs

Run	ΔT (min)	PUX (%)	PUR (%)	RCX (%)	RCR (%)	SCX (l/g)	SCR (l/g)	PRX (g/h l_s)	PRR (g/h l_s)
A	2.55	74.0	93.8	96.0	66.6	2.47	3.57	2.27	1.58
B	2.75	93.0	96.2	97.3	91.6	2.44	2.59	2.31	2.17
C	2.80	95.6	95.4	95.0	96.1	2.48	2.45	2.27	2.30
D	3.05	91.5	70.9	61.5	94.7	3.86	2.51	1.46	2.24

Table 6
Experimental performance parameters for the three configurations (rotation period = 2.75 min)

Run	Configuration	PUX (%)	PUR (%)	RCX (%)	RCR (%)	SCX (l/g)	SCR (l/g)	PRX (g/h l_s)	PRR (g/h l_s)
1	2222	93.0	96.2	97.3	91.6	2.44	2.59	2.31	2.17
2	1331	94.8	95.0	97.1	96.8	2.45	2.45	2.30	2.29
3	1241	92.6	95.2	97.5	94.5	2.44	2.52	2.31	2.24

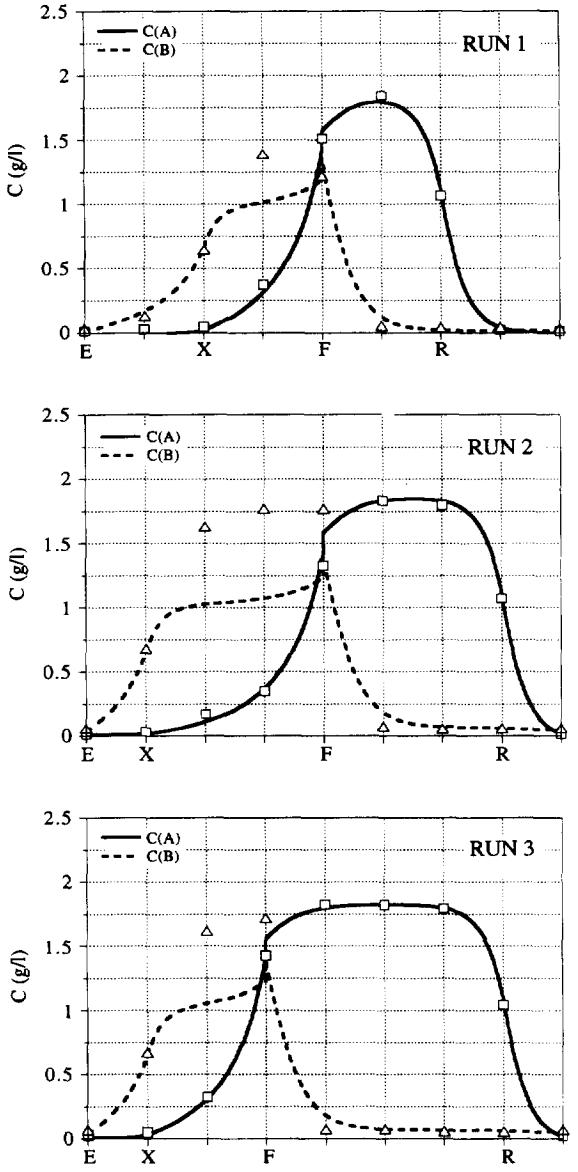

Fig. 8. Comparison between experimental (points taken at half time period in the cyclic steady state, SMB operation) and simulated (steady state TMB operation) internal profiles.

5. Conclusions

A model for predicting the cyclic steady state behavior of the SMB was developed using the corresponding TMB approach. This SMB package is an important learning and training tool used to predict the effect of operating variables on the process performance, and so the choice of the best conditions for the SMB operation.

The separation of bi naphthol enantiomers was carried out in a SMB pilot unit Licosep 12-26. Operating conditions for successful operation leading to high extract and raffinate purities as well as high recoveries were based on process simulation. Different configurations were also tested experimentally in the SMB pilot unit. For this system, no significant differences were observed in the performance parameters between the three configurations studied.

The SMB package was used to predict the SMB performance and the steady state internal profiles for the bi naphthol separation in good agreement with experimental results.

6. Symbols

c_{ij}	fluid phase concentration of component i in zone j
D_{Lj}	axial dispersion coefficient in the zone j
k	mass transfer coefficient
L_j	length of zone j
P_{ej}	Peclet number for zone j ($=v_jL_j/D_{Lj}$)
PRR	productivity for the raffinate
PRX	productivity for the extract
PUR	purity of the raffinate
PUX	purity of the extract
Q_j	volumetric liquid flow-rate in zone j
Q_s	solid flow-rate

q_{ij} average adsorbed phase concentration of component i in zone j
q_{ij}^* adsorbed concentration of component i in zone j in equilibrium with c_{ij}
RCR recovery of A in the raffinate
RCX recovery of B in the extract
SCR solvent consumption for the raffinate
SCX solvent consumption for the extract
t time
u_s solid velocity
V_s volume of the solid-phase, m^3
v_j interstitial fluid velocity in the zone j
z axial coordinate

6.1. Greek symbols

α_j number of mass transfer units $(=kL_j/u_s)$
ε bed porosity
γ_j ratio between fluid and solid velocities $(=v_j/u_s)$
γ_{ij}^* dimensionless parameter $(=\gamma_j \varepsilon c_{ij}/(1-\varepsilon)q_{ij})$

6.2. Subscripts and superscripts

A less retained component
B more retained component
E eluent
F feed
R raffinate
X extract

Acknowledgments

Financial support from the European Community under the BRITE-EURAM Programme (Contract No. BRE2-CT92-0337) is gratefully acknowledged. Thanks are also due to R.M. Nicoud and J. Blehaut (Separex) and J. Kinkel (Merck) for helpful discussions and preparation of the chiral packing.

References

[1] D.B. Broughton, US Pat. 2 985 589 (1961).
[2] A.J. de Rosset, R.W. Neuzil and D.B. Broughton, in A.E. Rodrigues and D. Tondeur (Editors), NATO ASI Percolation Processes, Theory and Applications, Sijthoff and Noordhoff, 1981.
[3] J.A Johnson, in A.E. Rodrigues et al. (Editors), NATO ASI Adsorption: Science and Technology, Kluwer, 1989.
[4] J.A Johnson and R.G. Kabza, in G. Ganetsos and P.E. Barker (Editors), Preparative and Production Scale Chromatography, Marcel Dekker, New York, 1993.
[5] D.B. Broughton, Chem. Eng. Prog., 64 (1968) 60.
[6] D.B Broughton, Chem. Eng. Prog., 66 (1970) 70.
[7] D.B. Broughton, Sep. Sci. Tech., 19 (1984) 723.
[8] A.J. de Rosset, R.W. Neuzil, D. Tajbl and J. Braband, Sep. Sci. Tech., 15 (1980) 637–653.
[9] J.L. Humphrey, Chem. Eng. Prog., 31–41, Oct. 1995.
[10] M.J. Gattuso, B. McCulloch and J.W. Priegnitz, presented at the symposium Chiral Europe, 1994.
[11] M.J. Gattuso, B. McCulloch, D.W. House and W.M. Baumann, presented at the symposium Chiral USA, 1995.
[12] R.M. Nicoud, LC·GC Int., 5 (1992) 43.
[13] G.E. Keller II, Chem. Eng. Prog., 56–67, Oct 1995.
[14] R.A. Sheldon, Chirotechnology: Industrial Synthesis of Optically Active Compounds, Marcel Dekker, New York, 1993.
[15] R.M. Nicoud, Simulated Moving Bed: Basics and Applications, European Meeting, Nancy, 1993.
[16] S.C. Stinton, C and EN, 44–74, Oct 1995.
[17] B. Balannec and G. Hotier, in G. Ganetsos and P.E. Barker (Editors), Preparative and Production Scale Chromatography, Marcel Dekker, New York, 1993.
[18] K. Gottschall, M. Kay and J. Reusch, presented at the 11th International Symposium on Preparative and Industrial Chromatography, Baden-Baden, Germany, 1994.
[19] M. Negawa and F. Shoji, J. Chromatogr., 590 (1992) 113.
[20] C.B. Ching, B.G. Lim, E.J.D. Lee and S.C. Ng, J. Chromatogr., 634 (1993) 215.
[21] H.W. Dandekar, A.K. Chandhok and J.W. Priegnitz, in Proceedings of the Fifth International Conference on Fundamentals of Adsorption, USA, 1995.
[22] G. Fuchs, R.M. Nicoud and M. Bailly, in M. Perrut (Editor), Proceedings of the 9th International Symposium on Preparative and Industrial Chromatography, Soc. Française de Chimie, Nancy, 1992.
[23] R.M. Nicoud, G. Fuchs, E. Kusters, F. Antia, R. Reuille and E. Schmid, in 3rd International Symposium on Chiral Discrimination, Tubigen, 1992.
[24] R.M. Nicoud, G. Fuchs, P. Adam, M. Bailly, E. Kusters, F. Antia, R. Reuille and E. Schmid, Chirality, 5 (1993) 267–271.
[25] A.E. Rodrigues, Z.P. Lu, J.M. Loureiro and L.S. Pais, J. Chromatogr. A, 702 (1995) 223.
[26] A.E. Rodrigues, J.M. Loureiro, Z.P. Lu, and L.S. Pais, in Proceedings of the Fifth International Conference on Fundamentals of Adsorption, USA, 1995.
[27] L.S. Pais, J.M. Loureiro and A.E. Rodrigues, Chem. Eng. Sci., 52 (1997) 245.
[28] D.M. Ruthven and C.B. Ching, Chem. Eng. Sci., 44 (1989) 1011.
[29] R.M. Nicoud, personal communication, 1995.
[30] R.M. Nicoud and A. Seidel-Morgenstern, in Simulated Moving Bed: Basics and Applications, Institut National Polytechnique de Lorraine, Nancy, 1993.

[31] N. Madsen and R. Sincovec, ACM Trans. Math. Soft., 5 (1979) 326.
[32] G. Storti, M. Mazzotti, M. Morbidelli and S. Carrà, AIChE J., 39 (1993) 471.
[33] M. Mazzotti, G. Storti and M. Morbidelli, AIChE J., 40 (1994) 1825.
[34] G. Storti, R. Baciocchi, M. Mazzotti and M. Morbidelli, Ind. Eng. Chem. Res., 34 (1995) 288–301.